Available online at www.sciencedirect.com
SCIENCE DIRECT®
Journal of Organometallic Chemistry 671 (2003) 101–112
Journal of Organometallic Chemistry
www.elsevier.com/locate/jorganchem

Origin of variation in polymerization activity for Ziegler–Natta catalyst with chloride and alkoxy ligands: a density functional study

Sumit Bhaduri [a,*], Sami Mukhopadhyay [b], Sudhir A. Kulkarni [b,*]

[a] Reliance Industries Limited, Chitrakoot 1st Floor, Sri Ram Mills, Worli, Mumbai 400 013, India
[b] Mahindra British Telecom Limited, Sharda Centre, Survey No. 91, CTS No. 11/B/1, Erandwane, Pune 411 004, India

Received 4 October 2002; received in revised form 9 January 2003; accepted 9 January 2003

Abstract

The origin of variation in the activity of Ziegler–Natta (ZN) catalysts having chloride and alkoxy ligands for ethylene and propylene polymerization has been investigated using density functional calculations at B3LYP/LANL2DZ level. The barriers for olefin insertion into $[TiCl_2CH_3]^+$ for ethylene and propylene are comparable whereas for catalysts with alkoxy ligands, the insertion barriers for propylene are about 5 kcal mol^{-1} higher than the corresponding ethylene insertion barriers. This supports the experimental observation that the propylene polymerization with ZN catalyst having alkoxy ligands has very low catalytic activity as compared to that for ethylene polymerization whereas $[TiCl_2CH_3]^+$ polymerizes both ethylene and propylene. It is further revealed that the electronic factors of ligands are dominant over the steric factors in olefin polymerization using such catalysts. The bonding aspects of various stationary structures on the potential energy surface of olefin insertion reaction are investigated using topological properties of electron density.

Keywords: Density functional; Ziegler–Natta catalysts; Activation energy; Olefin polymerization; Alkoxy ligands; Electron density

1. Introduction

Polyethylene and polypropylene are two of the largest volume commodity plastic with a total global production in excess of 72 billion kilogram [1]. The catalysts used in the manufacture of these two polyolefins play a very important role in the productivity and overall properties of the final polymer and are estimated to have a global market [2] of $1.5bn. In spite of the spectacular advances in metallocene and other single site catalysts in recent times, the commercial manufacture of polypropylene and high-density polyethylene is still largely based on magnesium chloride supported titanium catalysts, in combination with suitable organo aluminum cocatalysts. The synthesis and performance of these catalysts, commonly referred to as Ziegler–Natta catalysts, have been reported in numerous publications and patents.

Ziegler–Natta (ZN) catalyst has been one of the most widely used industrial catalyst for polymerization of olefins. Several experimental [3] and theoretical [4] investigations have been carried out using this catalyst. The commonly accepted mechanism of ZN catalysis is due to Cossee [5] wherein the active catalyst is assumed to have a vacant site to which monomer olefin binds to form metal–alkyl–olefin complex as shown in step 1 of Scheme 1. Further, olefin inserts into the metal alkyl bond through four center transition state leading to new alkyl complex of longer chain and generation of vacant site on the catalyst (cf. step 2 of Scheme 1). There exist a large number of theoretical studies addressing elementary steps in the reaction mechanism proposed by Cossee as well as those involving two component $TiCl_4$–AlR_3 system [6]. These studies have been based on various levels of theory using variety of basis-sets. However, essential features of the Cossee mechanism remain unchanged irrespective of level of theory and basis set [6,7].

* Corresponding authors.
E-mail addresses: sumit_bhaduri@ril.com (S. Bhaduri), samim@mahindrabt.com (S. Mukhopadhyay), sudhirk@mahindrabt.com (S. Kulkarni).

0022-328X/03/$ - see front matter © 2003 Elsevier Science B.V. All rights reserved.
doi:10.1016/S0022-328X(03)00049-4

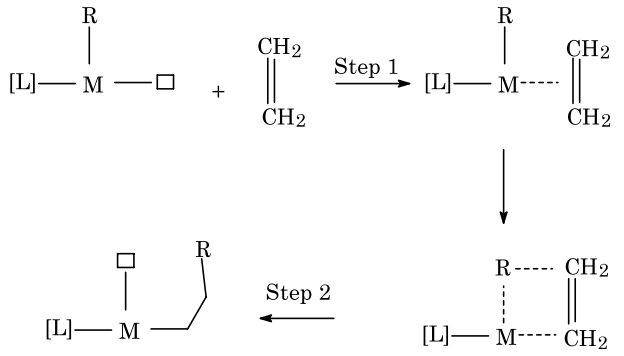

Scheme 1.

Using computational methods, the mechanism of alkene polymerization by classical Ziegler–Natta catalyst has been investigated by several authors. However to the best of our knowledge no semi quantitative, mechanistic studies have been carried out on the comparative activities of titanium haloalkoxy species towards the polymerization of ethylene and propylene. Such studies are of obvious importance since it is well established that alkoxy or haloalkoxy species show notably different activities in the polymerization of ethylene and propylene. Thus while alkoxy or haloalkoxy species are known to be active catalysts for ethylene polymerization, they show little or no activity in the polymerization of propylene [8]. In fact because of this adverse effect on activity, in the manufacture of polypropylene catalyst using $Mg(OEt)_2$ as the precursor, the removal of $Ti(OEt)Cl_3$ is extremely important for a catalyst of high activity [9]. The work reported here was undertaken with a view to offer an explanation for these technologically important empirical observations. In the present work, we assume the reaction mechanism due to Cossee and investigate differences in the reaction profiles of $TiCl_4$ and $Ti(OR)_4$ catalyzed ethylene and propylene polymerization.

2. Methodology

The active catalysts (having one vacant site as suggested by Cossee) selected for this work are $[TiCl_2CH_3]^+$, $[Ti(OCH_3)_2CH_3]^+$ and $[Ti(O-{}^tBu)_2CH_3]^+$. We have also studied a model active catalyst $[TiCl(OCH_3)CH_3]^+$ to understand the effect of replacing one of the chloride ligands by OCH_3 group. All the geometries have been obtained using hybrid density functional method B3LYP [10] (three parameter Becke's exchange energy functional along with correlation functional due to Lee, Yang and Parr). The LANL2DZ basis set which includes a double zeta valence basis set (8s5p5d)/[3s3p2d] for Ti with the Hay and Wadt ECP replacing core electrons up to 2p and Huzinaga–Dunning double zeta basis set for all other atoms has been used throughout the calculations. The vibrational frequencies and zero-point energies (ZPE) of all the stationary points have been obtained (cf. Table 1).

Some of the mechanistic aspects of the catalytic process have been investigated on the basis of the bonding features of all the structures obtained from topological analysis of electron density. All the calculations have been performed using ab initio program Gaussian 94 [11].

3. Results and discussion

All the stationary structures of reactants viz. active catalysts and olefins are displayed in Fig. 1. We initiate our study (using the level of theory discussed above) with ethylene and propylene polymerization using $[TiCl_2CH_3]^+$ as an active catalyst, although there are several reports on ab initio and density functional investigations on this [7]. The stationary structures on the potential energy surface (PES) of ethylene and propylene polymerization are found to be similar to earlier reported structures [7] and hence not reported herein. The relative energies for ethylene and propylene insertion reactions for different catalysts studied herein are shown in Table 1. The active catalyst, $[TiCl_2CH_3]^+$ has one vacant site for olefin attack and the ethylene complex has two structures with one having ethylene and $Ti–CH_3$ parallel to each other and the other where they are almost perpendicular. The former ethylene complex is stabilized by 37.98 kcal mol^{-1} compared to reactants (ethylene + active catalyst) and ethylene carbons are at the distances of 2.302 and 2.855 Å from Ti. The C=C bond of ethylene gets elongated from 1.348 Å in the reactant to 1.373 Å in the complex. In the TS, the C=C of ethylene as well as $Ti–CH_3$ bonds elongate and new Ti–C(ethylene) and $Ti–CH_3\cdots CH_2=CH_2$ bonds are being formed. The $Ti\cdots H(CH_3)$ distance in the TS is 2.046 Å and the corresponding C–H bond is longer than other hydrogens in that CH_3 implying stabilization of TS due to agostic interaction [4,6]. The geometrical parameters reported herein are similar to those by Bernardi et al. using B3LYP/MIDI4 level of theory [6]. The barrier for ethylene insertion reaction is about 8.06 kcal mol^{-1}, which is similar to values reported earlier [7]. For propylene, the complex exhibits two structures: one having methyl group of propylene *syn* to $Ti–CH_3$ bond and the other *anti* to $Ti–CH_3$ bond with stabilization of 40.99 and 48.28 kcal mol^{-1}, respectively. The propylene carbons are at distances of 2.336 and 2.732 Å from Ti in the *syn* complex whereas they are 2.234 and 2.929 Å in the *anti* complex. The TS also has two possibilities with *syn* TS being more stabilized than the *anti* TS (activation barrier of 7.15 kcal mol^{-1} as against 17.87 kcal mol^{-1}, respectively). The relative energy profile for ethylene and propylene insertion in

Table 1
Zero-point energy (ZPE) corrected relative energies (kcal mol^{-1}) of stationary points on the PES of ethylene and propylene polymerization using different catalysts at B3LYP/LANL2DZ level

Active catalyst	Olefin	E (complex)	E (TS)	E_{act} [a]	E (product)
$[TiCl_2CH_3]^+$	C_2H_4	−37.98	−29.92	8.06	−42.49
	C_3H_6 (*syn*)	−40.99	−33.84	7.15	−42.05
	C_3H_6 (*anti*)	−48.28	−30.41	17.87	−43.66
$[TiCl(OMe)CH_3]^+$	C_2H_4	−30.97	−22.57	8.40	−35.94
	C_3H_6 (*syn*, Cl)	−39.04	−25.09	13.95	−34.39
	C_3H_6 (*anti*, Cl)	−38.99	−21.73	17.26	−34.87
	C_3H_6 (*anti*, OMe)	−39.00	−21.92	17.07	−35.77
$[Ti(OMe)_2CH_3]^+$	C_2H_4	−26.00	−16.85	9.15	−30.50
	C_3H_6 (*syn*)	−32.03	−18.25	13.78	−28.76
	C_3H_6 (*anti*)	−31.85	−14.68	17.17	−28.67
$[Ti(O-^tBu)_2CH_3]^+$	C_2H_4	−24.25	−15.12	9.13	−28.91
	C_3H_6 (*syn*)	−29.56	−15.77	13.79	−26.77
	C_3H_6 (*anti*)	−29.24	−12.15	17.09	−26.48

Total ZPE corrected energies (electronic+ZPE in au) of active catalysts and olefins are: $[TiCl_2CH_3]^+ = -127.647569$; $[TiCl(OMe)CH_3]^+ = -227.822619$; $[Ti(OMe)_2CH_3]^+ = -327.983798$; $[Ti(O-^tBu)_2CH_3]^+ = -563.699384$; $C_2H_4 = -78.526874$; $C_3H_6 = -117.811103$

[a] E_{act} is insertion barrier in kcal mol^{-1}.

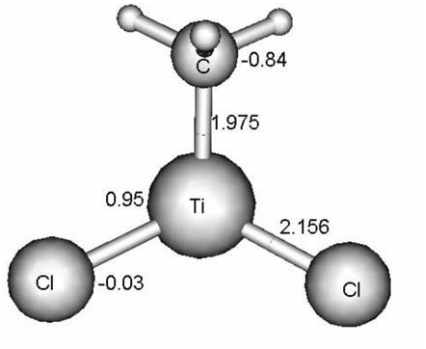

$[TiCl_2CH_3]^+$

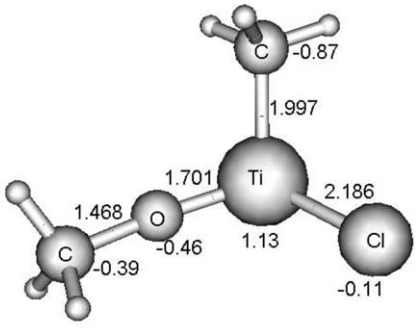

$[TiCl(OMe)CH_3]^+$ (**1a**)

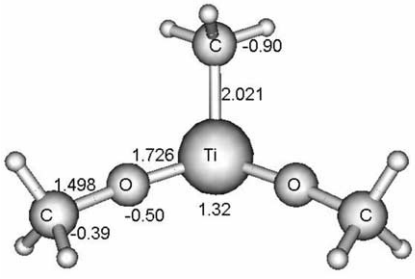

$[Ti(OMe)_2CH_3]^+$ (**2a**)

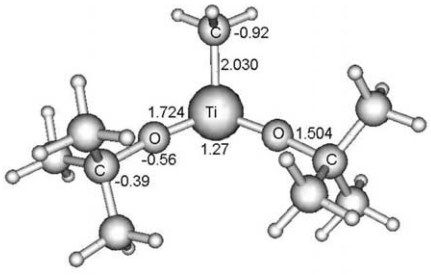

$[Ti(OtBu)_2CH_3]^+$ (**3a**)

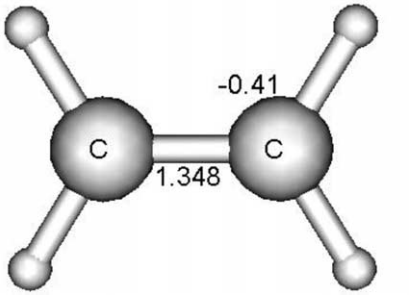

C_2H_4

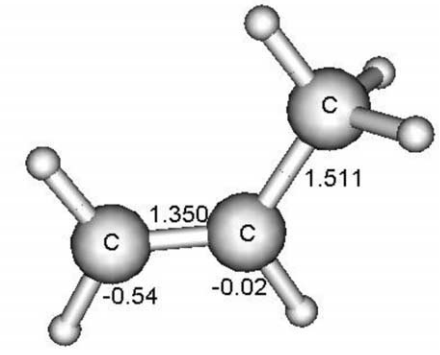

C_3H_6

Fig. 1. Geometrical parameters and Mulliken charges for active catalysts and olefins at B3LYP/LANL2DZ level. Bond lengths are in Å. All the structures have been visualized by using MSE_Pro molecular modeling software [19].

$[TiCl_2CH_3]^+$ is displayed in Fig. 2. Thus, both ethylene and propylene can be polymerized using this simple catalyst as they have similar activation barriers for olefin insertion.

We studied alkene insertion reaction with a model active catalyst $[TiCl(OCH_3)CH_3]^+$ (1a) wherein one of the chloride ligands of $[TiCl_2CH_3]^+$ has been replaced by methoxy group. This replacement gets reflected in (a) elongation of Ti–CH_3 bond by 0.022 Å. (b) Enhancement of positive Mulliken charge on Ti (1.13 compared to 0.95 as shown in Fig. 1). The active catalyst has almost linear Ti–O–CH_3 bond with angle of 169.7° as shown in Fig. 1 which is similar to the X-ray structure for $TiI(O–Ar)_3$ complex as well as $[TiCl_3OEt]_n$ [12]. All stationary points on the PES of ethylene and propylene polymerization pathways via $[TiCl(OCH_3)CH_3]^+$ catalyst are shown in Fig. 3. The ethylene complex (**1b**) is seen to be stabilized by 30.97 kcal mol^{-1} compared to reactants, and the ethylene insertion barrier is found to be 8.40 kcal mol^{-1} (cf. Table 1 and Fig. 4). Ti–ethylene distances in the ethylene complex (**1b**) are longer (2.379 and 2.840 Å) than those in the ethylene complex of $[TiCl_2CH_3]^+$. For propylene, four possibilities for the olefin complex exist: (a) Methyl group of propylene is *syn* to Ti–CH_3 bond and towards Cl group denoted as (*syn*, Cl); (b) methyl group of propylene is *syn* to Ti–CH_3 bond and towards OMe group denoted as (*syn*, OMe); (c) methyl group of propylene is anti to Ti–CH_3 bond and towards Cl group (*anti*, Cl); and (d) methyl group of propylene is *anti* to Ti–CH_3 bond and towards OMe group denoted as (*anti*, OMe). The complex a) is stabilized by 39.04 kcal mol^{-1} whereas complex b) was not found on the PES of reaction. The (*syn*, Cl) (**1e**) complex has propylene almost perpendicular to Ti–CH_3 bond with shortest Ti–C_3H_6 distance of 2.301 Å (cf. Fig. 3). Complexes c) **1h** and d) **1k** are stabilized by 38.99 and 39.00 kcal mol^{-1}, respectively. The corresponding barriers for propylene insertion through complexes **1e**, **1h** and **1k** are found to be 13.95 and 17.26 and 17.07 kcal mol^{-1}, respectively as shown in the relative energy profile diagram in Fig. 4. Thus, by replacing one of the chloride by methoxy group, a significant increase in the activation barrier is observed for propylene insertion compared to ethylene insertion. Further, the Ti–C_3H_6 bond is shorter in the TS of (*syn*, Cl) complex compared to other two possibilities (cf. **1f**, **1i** and **1l** in Fig. 3).

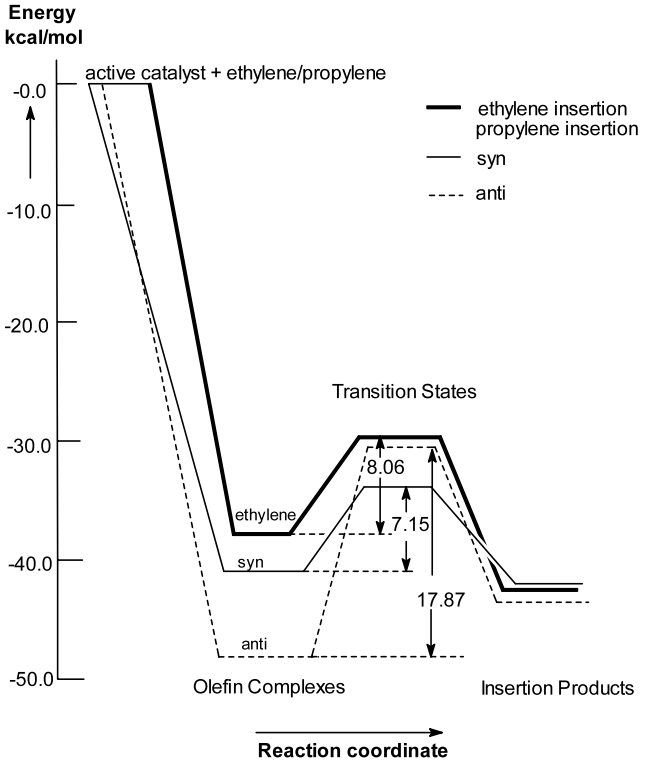

Fig. 2. Relative energy profile for ethylene and propylene insertion into $[TiCl_2CH_3]^+$ at B3LYP/LANL2DZ level after inclusion of zero-point energy correction.

A similar study was taken up on the system having $[Ti(OCH_3)_2CH_3]^+$ as an active catalyst (cf. **2a** in Fig. 1). Both Ti–CH_3 and Ti–O bonds become longer than in the $[TiCl(OCH_3)CH_3]^+$ catalyst. The Mulliken charge on Ti becomes further positive (1.32) after replacement of second chloride by OCH_3 (cf. Fig. 1). The optimized geometries for complexes, TSs and products for ethylene and propylene insertion into Ti–CH_3 bond are shown in Fig. 5 and corresponding relative energy profile is displayed in Fig. 6. The ethylene complex **2b** has ethylene almost perpendicular to Ti–CH_3 bond similar to the ethylene complex **1b**. In the corresponding TS, the short Ti···H(CH_3) distance (2.075 Å) and one long C–H bond of CH_3 (1.136 against 1.094 Å for the other C–H bonds) is indicative of agostic interaction [4,6]. The ethylene complex **2b** is stabilized by 26.00 kcal mol^{-1} and the barrier to ethylene insertion is 9.15 kcal mol^{-1}. The propylene complexes are formed with three different geometries, viz. methyl group of propylene is syn to Ti–CH_3 bond **2e**, methyl group of propylene is anti to Ti–CH_3 bond **2h** and the third where propylene is almost perpendicular to Ti–CH_3 bond (not shown in Fig. 5). The *syn* complex **2e** gets stabilized by 32.03 kcal mol^{-1} compared to reactants and has an insertion barrier of 13.78 kcal mol^{-1}. On the other hand, the *anti* complex **2h** is stabilized by 31.85 kcal mol^{-1} with an insertion barrier of 17.17 kcal mol^{-1} (cf. Fig. 6). Thus, when the alkoxy ligand is used instead of chloride, the barrier for propylene insertion is about 4–5 kcal mol^{-1} higher than that for ethylene. This would have significant effect on the turnover frequency for polypropylene production. From Figs. 3 and 5 it should be noted that all product structures have short Ti···CH_3 distance of the bond which gets broken in the insertion reaction implying that stabilization to the structure is gained through this interaction. Further, all product structures have two C–H bonds of methyl group having α-agostic interaction as indicated by short Ti···H(CH_3)

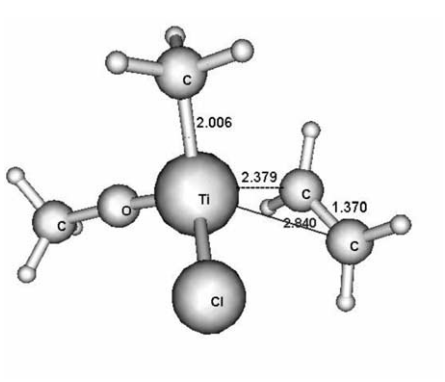

$[TiCl(OMe)CH_3\ldots C_2H_4]^+$ Complex (**1b**)

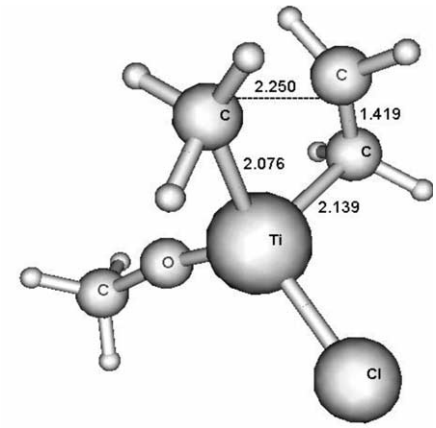

$[TiCl(OMe)CH_3\ldots C_2H_4]^+$ TS (**1c**)

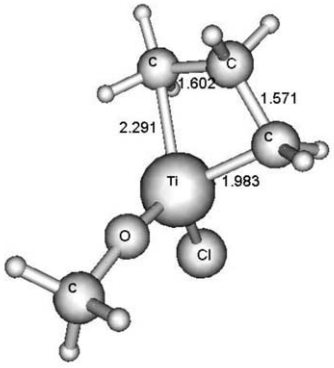

$[TiCl(OMe)C_3H_7]^+$ Product (**1d**)

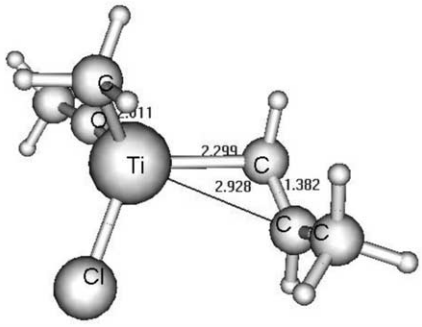

$[TiCl(OMe)CH_3\ldots C_3H_6]^+$ (syn, Cl) Complex (**1e**)

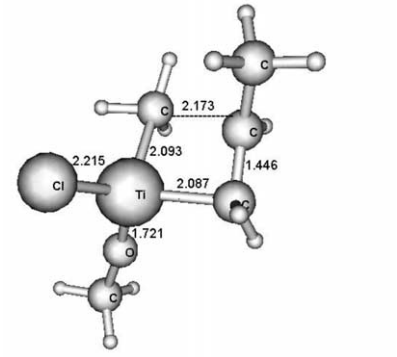

$[TiCl(OMe)CH_3\ldots C_3H_6]^+$ (syn, Cl) TS (**1f**)

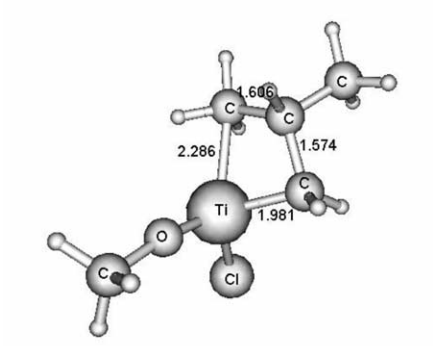

$[TiCl(OMe)C_4H_9]^+$ (syn, Cl) Product (**1g**)

Fig. 3. Optimized geometries of stationary points observed for ethylene and propylene insertion in $[TiCl(OMe)CH_3]^+$ active catalyst at B3LYP/LANL2DZ level. Bond lengths are in Å.

distances as well as corresponding longer C–H bonds having such interactions. Similar observations for product structures have been reported earlier in case of ethylene polymerization [4,6].

We also studied effect of using bulkier ligand like tertiary butoxy instead of methoxy (the optimized geometries are reported as supplementary information). The Mulliken charge on Ti in the active catalyst, $[Ti(O{-}^tBu)_2CH_3]^+$ does not change significantly compared to that in $[Ti(OCH_3)_2CH_3]^+$. The ethylene complex is stabilized by 24.25 kcal mol^{-1} whereas two propylene complexes, viz. *syn* and *anti* are respectively stabilized by 29.56 and 29.24 kcal mol^{-1}. The activation barrier for ethylene insertion is 9.13 kcal mol^{-1} and barriers for propylene insertion are found to be 13.79 and 17.09 kcal mol^{-1} for the syn and anti complexes, respectively (cf. Fig. 7). These barriers are similar to that for methoxy ligands, implying that bulk of ligands does not impart significant effect on the alkene insertion in $Ti–CH_3$ bond. The electronic effects introduced by replacement of chloride ligand by alkoxy ligand are significant and govern the reaction profiles.

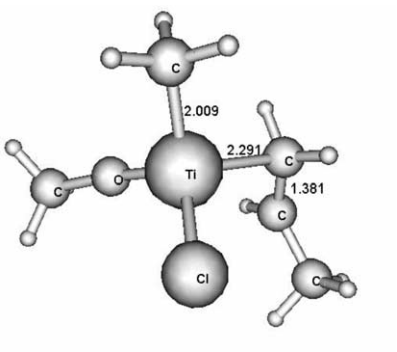

$[TiCl(OMe)CH_3\ldots C_3H_6]^+$ (Anti, Cl) Complex (**1h**)

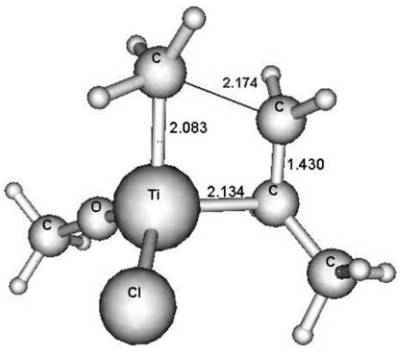

$[TiCl(OMe)CH_3\ldots C_3H_6]^+$ (Anti, Cl) TS (**1i**)

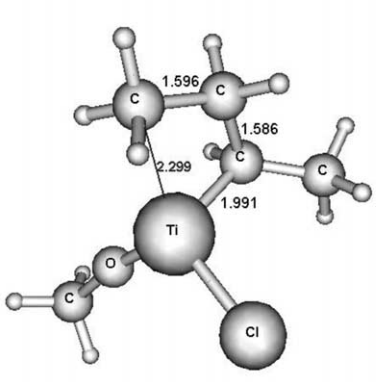

$[TiCl(OMe)C_4H_9]^+$ (Anti, Cl) Product (**1j**)

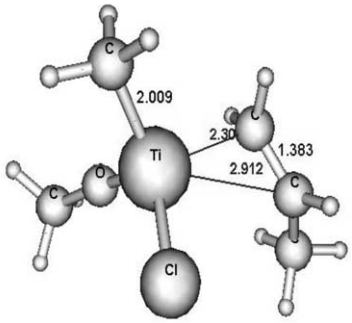

$[TiCl(OMe)CH_3\ldots C_3H_6]^+$ (Anti, OMe) Complex (**1k**)

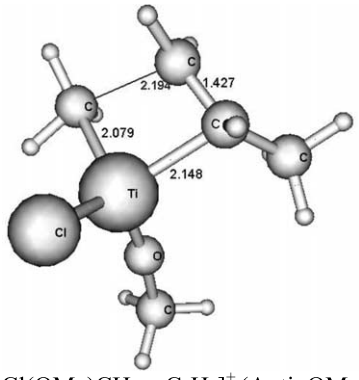

$[TiCl(OMe)CH_3\ldots C_3H_6]^+$ (Anti, OMe) TS (**1l**)

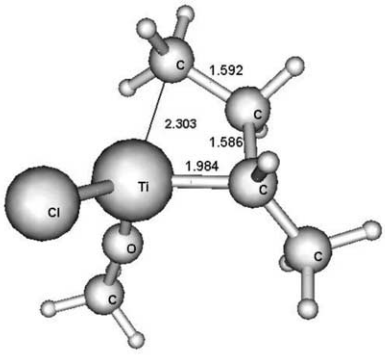

$[TiCl(OMe)C_4H_9]^+$ (Anti, OMe) Product (**1m**)

Fig. 3 (*Continued*)

Comparison of insertion barriers of ZN catalysts having chloride ligands with methoxy and tertiary butoxy ligands clearly reveal that the latter have significantly higher barriers for propylene insertion than for ethylene insertion (cf. Figs. 2, 6 and 7, and Table 1). This result is in accordance with the experimental observation that ZN catalysts with alkoxy ligands are not suitable for propylene polymerization [8]. Simple calculations for reaction rates based on activation barriers shows that the ZN catalysts with alkoxy ligands have the ethylene insertion rates faster by order of 10^3–10^4 than propylene (assuming constant pre-factor).

A careful analysis of Table 1 reveals that the ethylene insertion reaction considered from catalyst$\cdots C_2H_4 \rightarrow$ product is exothermic by about 5 kcal mol^{-1} irrespective of the catalyst used. On the other hand, the product formation is exothermic by about 1.06 kcal mol^{-1} only in the case of propylene insertion into $[TiCl_2CH_3]^+$ catalyst in *syn* fashion whereas the propylene insertion

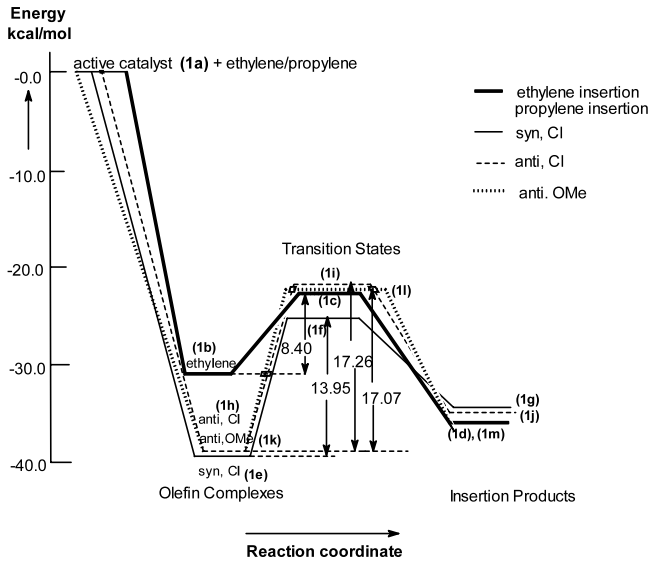

Fig. 4. Relative energy profile for ethylene and propylene insertion into $[TiCl(OCH_3)CH_3]^+$ at B3LYP/LANL2DZ level after inclusion of zero-point energy correction.

in *anti* fashion is endothermic. For all other catalysts, the propylene insertion is endothermic. This is a clear differentiating factor between conventional ZN catalysts and those having alkoxy ligands and could be a governing factor for the activity of olefin polymerization. Thus, exothermicity of reactions for different catalysts seems to have a direct bearing on the activation barrier, which is clearly reflected in higher insertion barriers for propylene than for ethylene in case of alkoxy ligands.

4. Electron density analysis

In order to understand bonding features of all the stationary points and electronic contributions of different ligands in alkene insertion into Ti–CH_3 bond, we have carried out topological analysis of electron density (ED). The topological analysis involves location and characterization of critical points (CP) in ED distribution and their interpretation [13]. The ED, Laplacian of ED and bond ellipticity are the parameters we have found to be useful for such analysis [14]. The negative Laplacian is an indicator of a covalent bond, whereas positive Laplacian indicates non-bonding or closed shell interaction between the two atoms [15]. The bond ellipticity defined from eigenvalues λ_i of the Hessian matrix of ED as $\varepsilon = (\lambda_1/\lambda_2 - 1)$ where λ_1 and λ_2 are magnitudes of negative eigenvalues with $\lambda_1 > \lambda_2$, is an indicator of the extent of double bond character. In addition, the bond ellipticity provides a measure of structural stability, the bonds with large ε values are prone to rupture [16]. A detailed topological analysis of ED involving location and characterization of all bond critical points (BCP) in ED distribution have been carried out for all the structures, however, only some of the representative parameters of some important stationary points are shown in Table 2. We have not reported ED analysis of stationary points of ethylene and propylene insertion for $[Ti(O{-}^tBu)_2CH_3]^+$ catalyst.

The ED analysis of all stationary structures on the reaction pathways for all the catalysts show expected features such as: BCP of all bonds with Ti show positive laplacian of ED. Ethylene/propylene complex shows a BCP between Ti and one of the carbons in double bond. This bond strengthens in the TS whereas Ti–CH_3 bond weakens and new bond formation (Ti)$CH_3\cdots$C (olefin) is clearly evident from emergence of new BCP. The product shows a complete formation of Ti–olefin bond and reduction in double bond character of olefinic bond as shown by the change in corresponding ellipticity (cf. Table 2) compared to ethylene complex and TS. The product also exhibits a weak bond between Ti and methyl carbon in which olefin insertion takes place.

Some general trends are noteworthy from reactions using different catalysts. The ED analysis of active catalysts reveals that Ti–CH_3 bond becomes weaker when OMe replaces every chloride. Similar trend is observed for Ti–CH_3 bond in case of ethylene complexes. The ethylene complex with $[TiCl_2CH_3]^+$ has higher ED in the Ti$\cdots C_2H_4$ bond (0.052 au) as compared to ethylene complexes of $[TiCl(OMe)CH_3]^+$ having ED of 0.043 and of $[Ti(OMe)_2CH_3]^+$ with ED of 0.037 au. The double bond character of C=C gets reduced in the ethylene complexes of all the catalysts as seen from their corresponding ED and ellipticity values at the BCP compared to those of ethylene (for ethylene C=C, ED = 0.312 au; $\varepsilon = 0.245$ and cf. Table 2). This may be indicative of the fact that forward donation from ethylene to Ti is more effective in $[TiCl_2CH_3]^+$ compared to other catalysts.

As seen earlier [4,6], the short Ti $\cdots$H(CH_3) distance and longer C–H of CH_3 attached to Ti are indicative of agostic interaction in olefin insertion TS and products. These observations are further supported by variation in electron density values at the BCP of C–H bonds involved. The ED values at BCP of such C–H bonds are lower than other C–H bonds of this methyl group. For example in the TS of ethylene insertion to $[Ti(OMe)_2CH_3]^+$ the ED value for C–H bond involved in agostic interaction is 0.223 au as against other C–H bonds having ED of 0.26 au (cf. Table 2). This is an indication of donation of ED from C–H bond to Ti. However, no bond is found between Ti$\cdots$.H(CH_3) in the TS and products, instead it is found to have BCP for Ti$\cdots CH_3$ bond (cf. Table 2). Thus, agostic interaction does not get reflected in the topology of electron density as in the case of conventional hydrogen bonds. Popelier and Logothetis [17] while characterizing the agostic

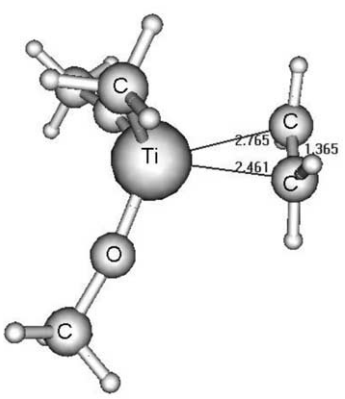

$[Ti(OMe)_2CH_3\ldots C_2H_4]^+$ Complex (**2b**)

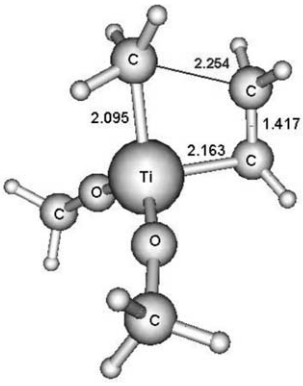

$[Ti(OMe)_2CH_3\ldots C_2H_4]^+$ TS (**2c**)

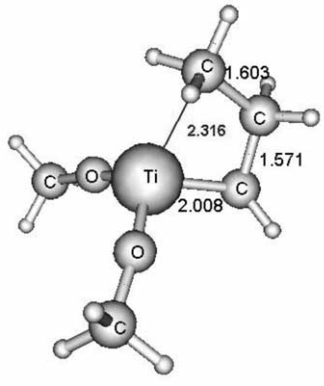

$[Ti(OMe)_2C_3H_7]^+$ Product (**2d**)

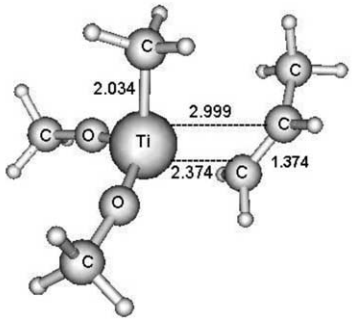

$[Ti(OMe)_2CH_3\ldots C_3H_6]^+$ Syn Complex (**2e**)

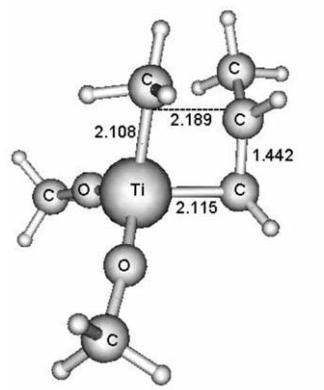

$[Ti(OMe)_2CH_3\ldots C_3H_6]^+$ Syn TS (**2f**)

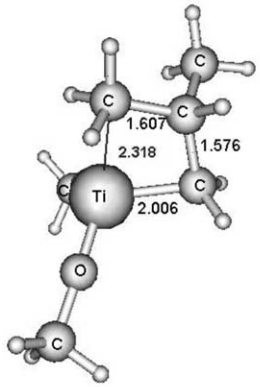

$[Ti(OMe)_2C_4H_9]^+$ Syn Product (**2g**)

Fig. 5. Optimized geometries of stationary points observed for ethylene and propylene insertion in $[Ti(OMe)_2CH_3]^+$ active catalyst at B3LYP/LANL2DZ level. Bond lengths are in Å.

bond on the basis of electron density drew similar conclusions.

Several experimental reports have attributed the better activity of $TiCl_4$ catalyst over $Ti(OR)_4$ due to electronegativity of chlorine leading to a more positive metal center [18]. However, we have found that the Mulliken charges on Ti of all the active catalysts (cf. Fig. 1) show opposite trend. This may be attributed to the more ionic nature of Ti–O bond as compared to Ti–Cl bond as is revealed by the more positive Laplacian of ED at the corresponding BCPs (cf. Table 2).

In an attempt to understand the differences between the ethylene and propylene insertion in $Ti–CH_3$ bond of different catalysts, a comparison of their abilities in bond formation with olefins is noteworthy. A comparison of ED at the Ti···olefin BCP for ethylene and propylene complexes shows that $Ti\cdots C_3H_6$ bond is weaker than $Ti\cdots C_2H_4$ bond in $[TiCl_2CH_3\cdots Olefin]^+$

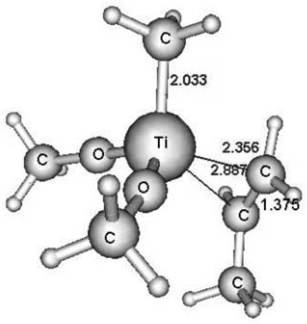

$[Ti(OMe)_2CH_3\ldots C_3H_6]^+$ Anti Complex (**2h**)

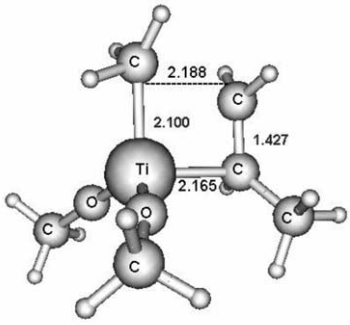

$[Ti(OMe)_2CH_3\ldots C_3H_6]^+$ Anti TS (**2i**)

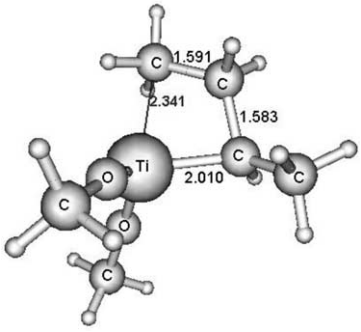

$[Ti(OMe)_2C_4H_9]^+$ Anti Product (**2j**)

Fig. 5 (*Continued*)

whereas $Ti\cdots C_3H_6$ bond is stronger than $Ti\cdots C_2H_4$ bond in complexes of all other catalysts (cf. Table 2). This observation is reflected in the relative stabilization of propylene complexes as compared to ethylene complexes (cf. Table 1 for relative energies of most favorable energy profiles using different catalysts). The propylene complexes are typically more stabilized by about 5–7 kcal mol^{-1} than the ethylene complexes for all the catalysts having one or more alkoxy ligand. However this stabilization is less in the case of $[TiCl_2CH_3]^+$. This is another differentiating factor that may be responsible for variation of activity towards propylene compared to ethylene.

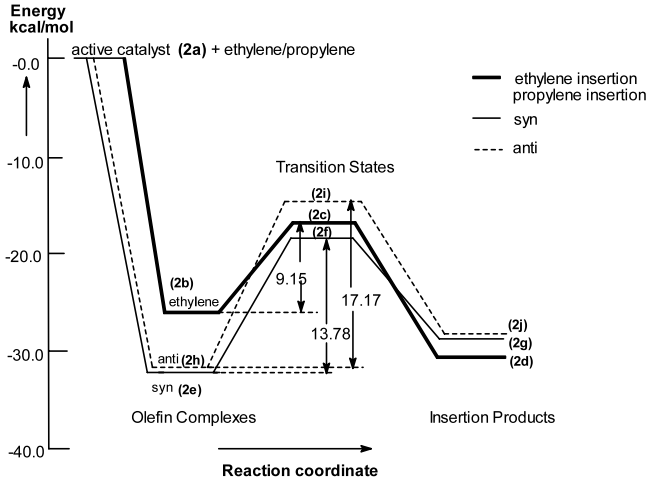

Fig. 6. Relative energy profile for ethylene and propylene insertion into $[Ti(OCH_3)_2CH_3]^+$ at B3LYP/LANL2DZ level after inclusion of zero-point energy correction.

5. Concluding remarks

An attempt has been made to understand the variation in the activity of Ziegler–Natta catalysts having chloride and alkoxy ligands for ethylene and propylene polymerization. Density functional calculations at B3LYP/LANL2DZ level reveal several important factors that may govern the variation in the ethylene Vs propylene polymerization activity for these catalysts. The barriers for olefin insertion into $[TiCl_2CH_3]^+$ for ethylene and propylene are comparable indicating that both reactions are feasible as per experimental observations. However for catalysts with alkoxy ligands, the insertion barriers for propylene are about 5 kcal mol^{-1} higher than the corresponding ethylene insertion barriers. This trend is seen in the catalysts with different

Table 2
Electron density and Laplacian of Electron density and bond ellipticities at some bond critical points (BCP) of $[TiL_1L_2CH_3]^+$ catalysts having different ligands at the B3LYP/LANL2DZ level geometry (L_1, L_2 being Cl or OMe)

Molecule	Location of CP in the specified bond	$\rho(r)$	$\nabla^2\rho(r)$	ε
$[TiCl_2CH_3]^+$	Ti–Cl	0.096	0.281	0.075
	Ti–CH_3	0.137	0.009	0.016
$[TiCl_2CH_3\cdots C_2H_4]^+$	Ti–CH_3	0.135	0.022	0.020
Complex	Ti$\cdots C_2H_4$	0.052	0.092	0.011
	C=C	0.300	−0.825	0.141
$[TiCl_2CH_3\cdots C_2H_4]^+$	Ti–CH_3	0.103	0.120	0.030
TS	Ti$\cdots C_2H_4$	0.091	0.063	0.039
	C=C	0.275	−0.686	0.097
	$C_2H_4\cdots CH_3$	0.051	0.061	0.25
$[TiCl_2C_3H_7]^+$	Ti–CH_3	0.055	0.172	0.042
Product	Ti$\cdots C_2H_4$	0.135	0.042	0.001
	C=C	0.201	−0.318	0.025
	C–C	0.186	−0.258	0.013
$[TiCl_2CH_3\cdots C_3H_6]^+$	Ti–CH_3	0.133	0.021	0.014
Syn complex	Ti$\cdots C_3H_7$	0.049	0.085	0.171
	C=C	0.302	−0.829	0.149
$[TiCl_2CH_3\cdots C_3H_6]^+$	Ti–CH_3	0.134	0.025	0.014
Anti complex	Ti$\cdots C_3H_7$	0.064	0.096	0.026
	C=C	0.293	−0.779	0.139
$[TiCl_2CH_3\cdots C_3H_6]^+$	Ti–CH_3	0.097	0.139	0.062
Syn TS	Ti$\cdots C_3H_7$	0.105	0.055	0.051
	C=C	0.262	−0.616	0.080
	$C_3H_7\cdots CH_3$	0.060	0.059	0.218
$[TiCl_2CH_3\cdots C_3H_6]^+$	Ti–CH_3	0.101	0.126	0.022
Anti TS	Ti$\cdots C_3H_7$	0.094	0.051	0.049
	C=C	0.271	−0.667	0.096
	$C_3H_7\cdots CH_3$	0.059	0.062	0.198
$[TiCl_2C_4H_9]^+$	Ti–CH_3	0.056	0.174	0.037
Syn product	Ti$\cdots C_3H_7$	0.136	0.045	0.006
	C=C	0.200	−0.312	0.037
	$C_3H_7\cdots CH_3$	0.185	−0.249	0.029
$[TiCl_2C_4H_9]^+$	Ti–Cl	0.091	0.280	0.095
Anti product	Ti–CH_3	0.052	0.169	0.166
	C=C	0.196	−0.288	0.048
	$C_3H_7\cdots CH_3$	0.193	−0.290	0.025
$[TiCl(OMe)CH_3]^+$ (**1a**)	Ti–Cl	0.089	0.266	0.059
	Ti–O	0.172	1.079	0.057
	O–CH_3	0.189	−0.029	0.001
$[TiCl(OMe)CH_3\cdots C_2H_4]^+$	Ti–CH_3	0.129	0.038	0.033
Complex (**1b**)	Ti$\cdots C_2H_4$	0.043	0.087	0.195
	C=C	0.302	−0.829	0.154
$[TiCl(OMe)CH_3\cdots C_2H_4]^+$	Ti–CH_3	0.096	0.125	0.035
TS (**1c**)	Ti$\cdots C_2H_4$	0.087	0.071	0.054
	(Ti)$CH_3\cdots C_2H_4$	0.053	0.059	0.189
	C=C	0.274	−0.683	0.109
$[TiCl(OMe)C_3H_7]^+$	Ti–CH_3	0.048	0.157	0.053
Product (**1d**)	Ti$\cdots C_2H_4$	0.130	0.056	0.027
	(Ti)$CH_3\cdots C_2H_4$	0.202	–0.325	0.038
	C=C	0.191	−0.280	0.018
$[TiCl(OMe)CH_3\cdots C_3H_6]^+$	Ti–CH_3	0.127	0.039	0.030
(*syn*, Cl) Complex (**1e**)	Ti$\cdots C_3H_6$	0.053	0.096	0.104
	C=C	0.297	−0.800	0.159
$[TiCl(OMe)CH_3\cdots C_3H_6]^+$	Ti–CH_3	0.090	0.136	0.048
(*syn*, Cl) TS (**1f**)	Ti$\cdots C_3H_6$	0.099	0.065	0.070
	(Ti)$CH_3\cdots C_3H_6$	0.061	0.057	0.185
	C=C	0.263	−0.619	0.094
$[TiCl(OMe)C_4H_9]^+$	Ti$\cdots C_3H_6$	0.131	0.053	0.027
(*syn*, Cl) Product (**1g**)	C=C	0.203	−0.328	0.031
	Ti–CH_3	0.048	0.157	0.082
	(Ti)$CH_3\cdots C_3H_6$	0.191	−0.279	0.012
$[TiCl(OMe)CH_3\cdots C_3H_6]^+$	Ti–CH_3	0.128	0.039	0.030

Table 2 (*Continued*)

Molecule	Location of CP in the specified bond	ρ(r)	$\nabla^2\rho$(r)	ε
(*anti*, Cl) Complex (**1h**)	Ti···C_3H_6	0.055	0.098	0.040
	C=C	0.298	−0.802	0.159
$[TiCl(OMe)CH_3\cdots C_3H_6]^+$	Ti–CH3	0.128	0.039	0.031
(*anti*, OMe) Complex (**1k**)	Ti···C_3H_6	0.054	0.095	0.049
	C=C	0.296	−0.795	0.158
$[Ti(OMe)_2CH_3]^+$ (**2a**)	Ti–O	0.161	1.015	0.044
	Ti–CH_3	0.124	0.045	0.017
	O–CH_3	0.198	−0.092	0.008
$[Ti(OMe)_2CH_3\cdots C_2H_4]^+$	Ti–CH_3	0.122	0.052	0.031
Complex (**2b**)	Ti···C_2H_4	0.037	0.083	0.063
	C=C	0.305	−0.846	0.166
$[Ti(OMe)_2CH_3\cdots C_2H_4]^+$	Ti–CH_3	0.091	0.129	0.029
TS (**2c**)	Ti···C_2H_4	0.081	0.076	0.032
	C=C	0.275	−0.684	0.121
	(Ti)$CH_3\cdots C_2H_4$	0.053	0.059	0.159
$[Ti(OMe)_2C_3H_7]^+$	Ti–CH_3	0.044	0.148	0.059
Product (**2d**)	Ti···C_2H_4	0.123	0.062	0.020
	C=C	0.203	−0.329	0.032
	(Ti)CH_3–C_2H_4	0.191	−0.280	0.076
$[Ti(OMe)_2CH_3\cdots C_3H_6]^+$	Ti–CH_3	0.121	0.056	0.030
Syn complex (**2e**)	Ti···C_3H_7	0.043	0.091	0.022
	C=C	0.301	−0.818	0.174
$[Ti(OMe)_2CH_3\cdots C_3H_6]^+$	Ti–CH_3	0.086	0.141	0.042
Syn TS (**2f**)	Ti···C_3H_7	0.093	0.076	0.058
	C=C	0.265	−0.626	0.112
	(Ti)$CH_3\cdots C_3H_7$	0.060	0.057	0.169
$[Ti(OMe)_2C_4H_9]^+$	Ti–CH_3	0.044	0.149	0.058
Syn product (**2g**)	Ti···C_3H_7	0.124	0.063	0.015
	C=C	0.203	−0.325	0.044
	(Ti)$CH_3\cdots C_3H_7$	0.191	−0.280	0.027

alkoxy ligands and is independent of bulk of ligands. This clearly supports the experimental observation that the propylene polymerization with ZN catalyst having alkoxy ligands has very low catalytic activity as compared to ethylene polymerization. The difference in the activation barrier for olefin insertion between ethylene and propylene is observed to be significant by replacement of one of the chlorides in $[TiCl_2CH_3]^+$ by alkoxy ligand. Further progressive replacement of chloride by alkoxy does not exhibit any major change in the insertion barriers. The use of bulkier ligands like O–^{t}Bu instead of O–Me does not show much change in the reaction profile (cf. Figs. 6 and 7). Thus, the electronic factors of ligands are dominant over the steric factors in olefin polymerization using such catalysts.

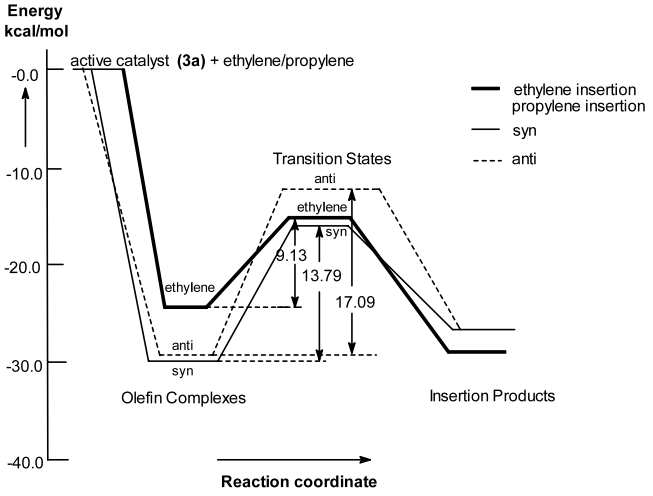

Fig. 7. Relative energy profile for ethylene and propylene insertion into $[Ti(O-^tBu)_2CH_3]^+$ at B3LYP/LANL2DZ level after inclusion of zero-point energy correction.

Further, the energies of olefin insertion reactions: catalyst···olefin complex → alkyl product show that ethylene insertion is exothermic irrespective of catalysts used. On the other hand, propylene insertion for similar reaction is exothermic only in case of $[TiCl_2CH_3]^+$. This observation may be a governing factor for activity variation of ethylene and propylene polymerization using Ti-based catalysts. The topological analysis of ED allows us to further understand the ED reorganization in various stationary structures of reaction profiles and suggests the relationship of ED with the activity variation.

Acknowledgements

The authors are grateful to Professor S.R. Gadre, University of Pune, India and to Dr. Libero Bartolotti, North Carolina Supercomputing Center, USA for providing computer facility. Financial support for this work was provided by Reliance Industries Limited. We thank the referee for useful suggestions.

References

[1] S.D. Ittel, L.K. Johnson, Chem. Rev. 100 (2000) 1169.
[2] J. Baker, European Chemical News, 20–26 March, 2000, p. 38.
[3] (a) G. Natta, P. Pino, V. Giannini, E. Mantica, M. Peraldo, Polym. Sci. 26 (1957) 120;
(b) D.S. Breslow, N.R. Newburg, J. Am. Chem. Soc. 81 (1959) 81;
(c) J.C.W. Chien, M.D. Rausch, W. Tsai, J. Am. Chem. Soc. 113 (1991) 8570;
(d) J.J. Eisch, S.I. Pombrik, G. Zheng, Organometallics 12 (1993) 3856 (and references therein).
[4] (a) H. Kawamura-Kuribayashi, N. Koga, K. Morokuma, J. Am. Chem. Soc. 114 (1992) 2359;
(b) J.C.W. Lorenz, T.K. Woo, T. Ziegler, J. Am. Chem. Soc. 117 (1995) 12793;
(c) T. Yoshida, N. Koga, K. Morokuma, Organometallics 14 (1995) 746.
[5] (a) P. Cossee, J. Catal. 3 (1964) 65;
(b) E.J. Arlman, P. Cossee, J. Catal. 3 (1964) 80;
(c) E.J. Arlman, P. Cossee, J. Catal. 3 (1964) 89;
(d) E.J. Arlman, P. Cossee, J. Catal. 3 (1964) 99.
[6] F. Bernardi, A. Bottoni, G.P. Miscione, Organometallics 17 (1998) 16.
[7] A.K. Rappe, W.M. Skiff, C.J. Casewit, Chem. Rev. 100 (2000) 1435 (and references therein).
[8] S.M. Pillai, M. Ravindranathan, S. Sivram, Chem. Rev. 86 (1986) 353.
[9] E. Albizzati, U. Giannini, G. Collina, L. Noristi, L. Resconi, in: E.P. Moore, Jr. (Ed.), Polypropylene Handbook, Hanser, New York, 1996, p. 23.
[10] (a) A.D. Becke, Phys. Rev. A 38 (1988) 3098;
(b) C. Lee, W. Yang, R.G. Parr, Phys. Rev. B 37 (1988) 785;
(c) A.D. Becke, J. Chem. Phys. 98 (1993) 5648.
[11] M.J. Frisch, G.W. Trucks, H.B. Schlegel, P.M.W. Gill, B.G. Johnson, M.A. Robb, J.R. Cheeseman, T. Keith, G.A. Petersson, J.A. Montgomery, K. Raghavachari, M.A. Al-Laham, V.G. Zakrzewski, J.V. Ortiz, J.B. Foresman, C.Y. Peng, P.Y. Ayala, W. Chen, M.W. Wong, J.L. Andres, E.S. Replogle, R. Gomperts, R.L. Martin, D.J. Fox, J.S. Binkley, D.J. Defrees, J. Baker, J.J.P. Stewart, M. Head-Gordon, C. Gonzalez, J.A. Pople, Gaussian 94, Revision B.3, Gaussian Inc., Pittsburgh, PA, 1995.
[12] (a) S.L. Satesky, J. Keddington, A.K. McMullen, I.P. Rothwell, J.C. Huffman, Inorg. Chem. 24 (1985) 995;
(b) M. Niemeyer, T.J. Goodwin, S.H. Risbud, P.P. Power, Chem. Mater. 8 (1996) 2745.
[13] R.F.W. Bader, Atoms in Molecules: a Quantum Theory, Clarendon, Oxford, 1990.
[14] S. Bhaduri, S. Mukhopadhyay, S.A. Kulkarni, J. Organomet. Chem. 654 (2002) 132.
[15] (a) R.G.A. Bone, R.F.W. Bader, J. Phys. Chem. 100 (1996) 10892;
(b) R.F.W. Bader, H. Essen, J. Chem. Phys. 80 (1984) 1943.
[16] (a) U. Koch, P.L.A. Popelier, J. Phys. Chem. 99 (1995) 9747;
(b) P.L.A. Popelier, J. Phys. Chem. 102 (1998) 1873.
[17] P.L.A. Popelier, G. Logothetis, J. Organomet. Chem. 555 (1998) 101.
[18] (a) V. Chandrasekhar, P.R. Srinivasan, S. Sivaram, Ind. J. Technol. 26 (1988) 53;
(b) A.W. Al-Sa'doun, Appl. Catal. A 105 (1993) 1.
[19] (a) MSE_Pro 1.0 Molecular Simulation Environment, Mahindra British Telecom Ltd., Pune, India, 2002. See also www.mahindrabt.com/services/cc_prod.htm;
(b) S.R. Gadre, in: J. Leszczynski (Ed.), Topography of Atomic and Molecular Scalar Fields in Computational Chemistry: Reviews of Current Trends, vol. 4, World Scientific, Singapore, 1999, pp. 1–53.